Juggling a Devil-Stick: Hybrid Orbit Stabilization Using the Impulse Controlled Poincaré Map

Nilay Kant and Ranjan Mukherjee, *Senior Member, IEEE*

***Abstract*—The control design for juggling a devil-stick between two symmetric configurations is proposed. Impulsive forces are applied to the devil-stick at the two configurations; and impulse of the force and its point of application are modeled as the control inputs. The dynamics of the devil-stick is described by a single return Poincaré map and it is shown that the control objective of juggling can be achieved by stabilizing a hybrid orbit. The impulse controlled Poincaré map (ICPM) approach, recently proposed for stabilization of continuous-time orbits of underactuated systems, is extended to achieve asymptotic stabilization of the hybrid orbit. The applicability of the ICPM approach to devil-stick juggling is demonstrated through numerical simulations.**

***Index Terms*—Devil-stick, hybrid orbit, orbital stabilization, impulsive control, juggling, Poincaré map, underactuated system.**

I. Introduction

The control problem of juggling an object in air has been investigated in the literature but these investigations have primarily focused on ball-juggling [2], [17]–[19], [21]. In one of the earliest studies [21], a ball was juggled by applying impulsive forces intermittently using a table with one degree-of-freedom. The approach was later extended [2] to develop a feedback control method for hybrid mechanical systems and simulations were used to demonstrate ball-juggling using a two degree-of-freeedom manipulator. The control problem of juggling a devil-stick is more challenging than that of juggling a ball since the orientation of the devil-stick has to be included in the dynamic model; in contrast, the ball has no orientation since it is modeled as a point mass.

Two hand-sticks are typically used to juggle a devil-stick and several different modes of juggling have been documented [5], [9]. Earlier works [15], [20] have proposed control designs for the mode of juggling known as *airplane-spin* or *propeller*; in this mode, a single hand-stick is used to rotate the devil-stick about a virtual horizontal axis using continuous-time inputs. For a human juggler, the simplest mode of juggling is *top-only idle*; it requires application of intermittent impulsive forces and is the subject of investigation of this letter. For top-only idle mode of juggling, a two-step control design was presented in [9]. In this work, a dead-beat controller was first designed to convert the nonlinear system into a controllable linear system. Depending upon initial conditions, the dead-beat controller may require a large input at the initial time and failure to apply the desired input may render the linear controller ineffective. To overcome this limitation, the control problem of top-only idle juggling is revisited here.

For top-only idle mode of juggling, the devil-stick model represents an underactuated system with three generalized coordinates and two control inputs. Importantly, it belongs to a special class of underactuated systems, that has received less attention, where the control inputs are purely impulsive and applied intermittently. The juggling task can be posed as a problem in orbital stabilization but a majority of the control methods developed for orbital stabilization use continuous inputs and are therefore rendered inapplicable. A new approach was recently proposed for orbital stabilization of a general class of underactuated systems [8]. In this approach, known as the Impulse Controlled Poincaré Map (ICPM), impulsive inputs are intermittently applied on a Poincaré section for stabilization of continuous-time orbits. Here, the ICPM approach is extended to stabilization of hybrid orbits in the context of the devil-stick juggling problem.

This letter is organized as follows. The control problem associated with the top-only idle mode of juggling is described in Section II. The recently developed mathematical model of the devil-stick [9] is presented in abridged form in Section III. The control design is presented in Section IV; it is based on linearization of the Poincaré map and is a perfect utilization of the ICPM approach. Numerical simulation results are provided in Section V. Section VI contains concluding remarks and future research directions.

II. Problem Description

A devil-stick that moves freely in a vertical plane has three degrees-of-freedom. The generalized coordinates associated with these degrees-of-freedom are shown in Fig. 1. They are comprised of the Cartesian coordinates of the center-of-mass $G \equiv (h_x, h_y)$, and orientation of the stick θ, measured counter-clockwise with respect to the horizontal. The stick is assumed

Manuscript received March 4, 2021; revised May 16, 2021; accepted June 12, 2021. Date of publication June 23, 2021; date of current version July 7, 2021. This work was supported by the U.S. National Science Foundation under Grant CMMI-1462118 and Grant CMMI-2043464. Recommended by Senior Editor J. Daafouz. *(Corresponding author: Ranjan Mukherjee.)*

The authors are with the Department of Mechanical Engineering, Michigan State University, East Lansing, MI 48824 USA (e-mail: mukherji@egr.msu.edu).

Digital Object Identifier 10.1109/LCSYS.2021.3091935

2475-1456 © 2021 IEEE. Personal use is permitted, but republication/redistribution requires IEEE permission.
See https://www.ieee.org/publications/rights/index.html for more information.

Authorized licensed use limited to: Michigan State University. Downloaded on January 05,2023 at 17:22:27 UTC from IEEE Xplore. Restrictions apply.

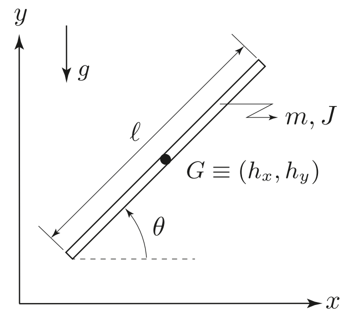

Fig. 1. A three degree-of-freedom devil-stick.

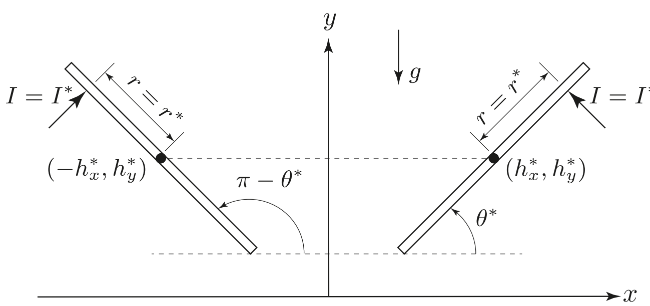

Fig. 2. Symmetric configurations of the devil-stick in Fig. 1.

to have length ℓ, mass m, and mass moment of inertia J about G. The objective is to juggle the stick between the symmetric configurations (θ^*, h_x^*, h_y^*) and $(\pi - \theta^*, -h_x^*, h_y^*)$ shown in Fig. 2, where $\theta^* \in (0, \pi/2)$. Impulsive forces are applied perpendicular to the devil-stick when its orientation is $\theta = \theta^*$ or $\theta = \pi - \theta^*$. A juggler is typically ambidextrous and the control actions at $\theta = \theta^*$ and $\theta = \pi - \theta^*$ are applied by hand sticks held in the right and left hands of the juggler. The control inputs are the pair (I, r), where $I, I \geq 0$, is the impulse of the impulsive force and r is the distance of the point of application of the force from G. The value of r is considered to be positive if the angular impulse of the impulsive force about G is positive when $\theta = \theta^*$, and negative when $\theta = \pi - \theta^*$. The steady-state values of the control inputs that juggle the stick between the symmetric configurations are denoted by the pair (I^*, r^*).

III. Devil-Stick Mathematical Model

A. Hybrid Dynamics

The dynamics of the devil-stick is described by the six-dimensional state vector X, where

$$X = \begin{bmatrix}\theta & \omega & h_x & v_x & h_y & v_y\end{bmatrix}^T, \ \omega \triangleq \dot{\theta}, \ v_x \triangleq \dot{h}_x, \ v_y \triangleq \dot{h}_y$$

Let t_k, $k = 1, 2, 3, \ldots$, denote the instants of time when the impulsive inputs are applied. Furthermore, let $k = (2n-1)$, $n = 1, 2, \ldots$, denote the instants of time when the impulsive inputs are applied by the hand stick held in the right hand; and $k = 2n$, $n = 1, 2, \ldots$, denote the instants of time when the impulsive inputs are applied by the hand stick held in the left hand. If t_k^- and t_k^+ denote the instants of time immediately before and after application of the impulsive inputs, the linear and angular impulse-momentum relationships can be used to describe the impulsive dynamics[1] [9]. We have for $k = 1, 3, 5, \ldots$:

$$X(t_k^+) = X(t_k^-) + \begin{bmatrix} 0 \\ (I_k r_k/J) \\ 0 \\ -(I_k/m)\sin\theta^* \\ 0 \\ (I_k/m)\cos\theta^* \end{bmatrix} \tag{1}$$

and for $k = 2, 4, 6, \ldots$

$$X(t_k^+) = X(t_k^-) + \begin{bmatrix} 0 \\ -(I_k r_k/J) \\ 0 \\ (I_k/m)\sin\theta^* \\ 0 \\ (I_k/m)\cos\theta^* \end{bmatrix} \tag{2}$$

where (I_k, r_k) denote the control inputs at time t_k.

For $t \in [t_k^+, t_{k+1}^-]$, $k = 1, 2, \ldots$, the devil-stick undergoes torque-free motion under gravity and its continuous-time dynamics is described by the differential equation [9]:

$$\dot{X} = \begin{bmatrix}\omega & 0 & v_x & 0 & v_y & -g\end{bmatrix}^T \tag{3}$$

where the initial condition $X(t_k^+)$ can be obtained from (1) or (2), depending on whether k is odd or even.

B. Half-Return Maps for Ambidextrous Juggler

For the hybrid dynamical system in Section III-A, we define two Poincaré sections S_r and S_l as follows [9]:

$$\begin{aligned} S_r &: \{X \in \mathbb{R}^6 | \theta = \theta^*\} \\ S_l &: \{X \in \mathbb{R}^6 | \theta = \pi - \theta^*\} \end{aligned} \tag{4}$$

Without loss of generality, it is assumed that the initial conditions are such that the trajectory of the devil-stick intersects S_r at $t = t_1$. Any point on S_r and S_l can be described by the vector Y:

$$Y = \begin{bmatrix}\omega & h_x & v_x & h_y & v_y\end{bmatrix}^T \tag{5}$$

The map $\mathbb{P}_r : S_r \to S_l$ can be determined from (1) and (3) as follows [9]:

$$Y(t_{k+1}^-) = A\,Y(t_k^-) + B_r \tag{6}$$

where the expressions for A and B_r can be found in [9] and $k = (2n-1)$, $n = 1, 2, \ldots$ Similarly, the map $\mathbb{P}_l : S_l \to S_r$ can be determined from (2) and (3) as follows [9]

$$Y(t_{k+1}^-) = A\,Y(t_k^-) + B_l \tag{7}$$

where the expressions for B_l can be found in [9] and $k = 2n$,

[1] Control designs for underactuated mechanical systems exploiting impulsive inputs can be found in [6]–[10], [14].

Authorized licensed use limited to: Michigan State University. Downloaded on January 05,2023 at 17:22:27 UTC from IEEE Xplore. Restrictions apply.

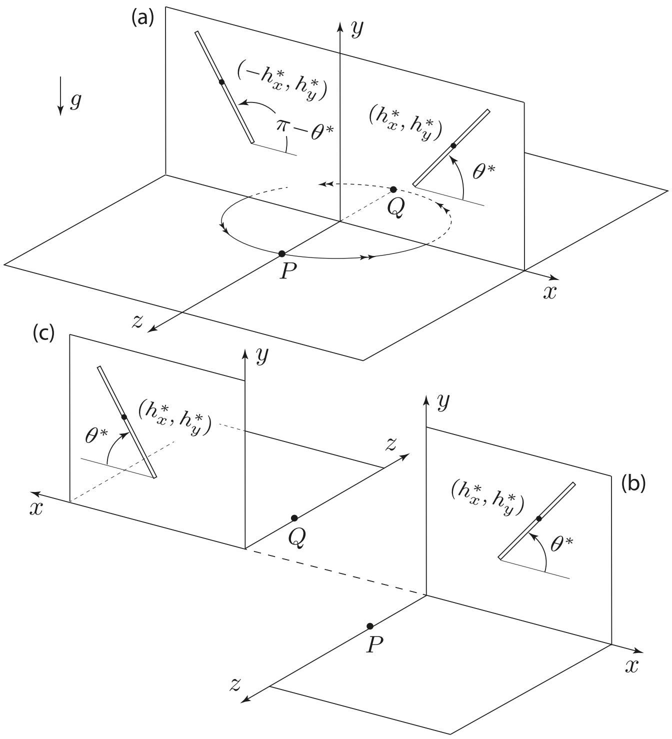

Fig. 3. (a) Ambidextrous juggler standing at P and applying control actions with both hands, (b) right-handed juggler standing at P and applying control action with right hand, (c) right-handed juggler standing at Q and applying control action with right hand.

$n = 1, 2, \dots$ Both $\mathbb{P}_r$ and $\mathbb{P}_l$ in (6) and (7) can be viewed as half-return maps [1], [4] since their composition are the return maps $\mathbb{P}_r \circ \mathbb{P}_l : S_l \to S_l$ and $\mathbb{P}_l \circ \mathbb{P}_r : S_r \to S_r$.

C. Single Return Map for Right-Handed Juggler

Let $z = 0$ denote the plane in which the devil-stick is juggled - see Fig. 3. An ambidextrous juggler stands at a point on the positive z axis, P in Fig. 3(a), and applies a control action with the right hand when $\theta = \theta^*$, and with the left hand when $\theta = \pi - \theta^*$. Instead of applying control actions using both right and left hands, the juggler can choose to apply all control actions using the right hand. This right-handed juggler will apply the control action standing at P when $\theta = \theta^*$ - see Fig. 3(b), and apply the next control action after changing location to Q when $\theta = \pi - \theta^*$ - see Fig. 3(c). It can be shown [9] that the Poincaré sections S_l and S_r are identical in the reference frame of the right-handed juggler, and equal to

$$S : \{X \in \mathbb{R}^6 | \theta = \theta^*\} \tag{8}$$

The half-return maps, $\mathbb{P}_r$ and $\mathbb{P}_l$ in (6) and (7), are also identical [9]. This implies that the hybrid dynamics of the devil-stick is described by a single return map $\mathbb{P} : S \to S$, which is given below [9]:

$$\omega(t_{k+1}^-) = -\omega(t_k^-) - (I_k r_k / J) \tag{9a}$$

$$h_x(t_{k+1}^-) = -h_x(t_k^-) - \big[v_x(t_k^-) - (I_k/m)\sin\theta^*\big]\delta_k \tag{9b}$$

$$v_x(t_{k+1}^-) = -v_x(t_k^-) + (I_k/m)\sin\theta^* \tag{9c}$$

$$h_y(t_{k+1}^-) = h_y(t_k^-) - (1/2) g\,\delta_k^2 + \big[v_y(t_k^-) + (I_k/m)\cos\theta^*\big]\delta_k \tag{9d}$$

$$v_y(t_{k+1}^-) = v_y(t_k^-) + (I_k/m)\cos\theta^* - g\,\delta_k \tag{9e}$$

where $\delta_k \triangleq (t_{k+1}^- - t_k^-)$, $k = 1, 2, \dots,$ is the time of flight between two consecutive control actions. During this time duration, the devil-stick rotates by a net angle $\pi - 2\theta^*$. Since the angular velocity of the stick remains constant in the interval $[t_k^+, t_{k+1}^-]$, δ_k is given as follows

$$\delta_k = \frac{\Delta\theta}{\omega(t_k^-) + (I_k r_k / J)}, \quad \Delta\theta \triangleq (\pi - 2\theta^*) \tag{10}$$

Let $\bar{Y}$ denote the state vector Y in the reference frame of the right handed juggler. Since δ_k in (10) is a function of state variables, the Poincaré map $\mathbb{P}$ in (9) can be written as

$$\bar{Y}(k+1) = \mathbb{P}\big[\bar{Y}(k), I(k), r(k)\big]$$
$$\bar{Y}(k) \triangleq \bar{Y}(t_k^-), \quad I(k) \triangleq I_k, \quad r(k) \triangleq r_k \tag{11}$$

The control design for juggling is presented next.

IV. Control Design

A. Steady-State Dynamics

It is clear from the discussion in Section III-C that the hybrid dynamics of the devil-stick can be described by the single Poincaré map $\mathbb{P}$ in the reference frame of the right-handed juggler. If the devil-stick undergoes the desired juggling motion, the system trajectories must pass through a fixed point on the Poincaré section S. If $\bar{Y}^* \triangleq [\omega^* \;\; h_x^* \;\; v_x^* \;\; h_y^* \;\; v_y^*]^T$ is the fixed point, it satisfies the relation

$$\bar{Y}^* = \mathbb{P}(\bar{Y}^*, I^*, r^*) \tag{12}$$

where (I^*, r^*) denote the steady-state values of the control inputs, defined in Section II. Using (9) and (10), the steady state values of the states and control inputs can be obtained as follows [9]:

$$\begin{aligned} \omega^* &= -\Delta\theta/\delta^*, & h_x^* &= g\delta^{*2}\tan\theta^*/4 \\ v_x^* &= g\tan\theta^*\delta^*/2, & v_y^* &= -g\,\delta^*/2 \\ I^* &= mg\delta^*/\cos\theta^*, & r^* &= 2J\cos\theta^*\Delta\theta/(mg\delta^{*2}) \end{aligned} \tag{13}$$

where δ^* denotes the steady-state value of δ and can be chosen by the user. For a given value of δ^*, the value of h_y^* can be chosen arbitrarily.

The desired juggling motion of the devil-stick is repetitive and can be described by the following hybrid orbit:

$$\mathcal{O}^* = \{X \in \mathbb{R}^6 | \bar{Y}(k) = \bar{Y}^*, I(k) = I^*, r(k) = r^*\} \tag{14}$$

In the next section, we discuss the problem of stabilization of the orbit $\mathcal{O}^*$, which implies stabilization of the juggling motion.

B. Stable Juggling - Stabilization of the Hybrid Orbit $\mathcal{O}^*$

The control inputs I^* and r^* ensure desired juggling motion of the devil-stick provided $\bar{Y}(t_1^-) = \bar{Y}^*$, i.e., the devil-stick configuration is at the fixed point at the time of the first control action. If this is not the case, the control inputs I^* and r^* may not converge the devil-stick trajectory to the desired orbit $\mathcal{O}^*$. Therefore, it is important to investigate the stability

Authorized licensed use limited to: Michigan State University. Downloaded on January 05,2023 at 17:22:27 UTC from IEEE Xplore. Restrictions apply.

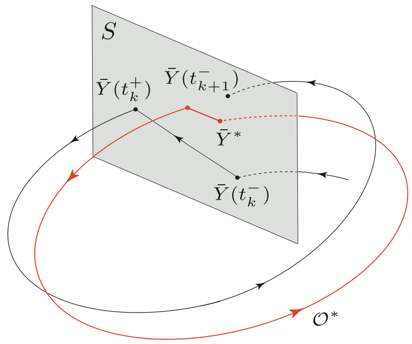

Fig. 4. Schematic of the ICPM approach to devil-stick juggling.

characteristics of $\mathcal{O}^*$. We first define an ϵ-neighborhood of $\mathcal{O}^*$ by

$$U_\epsilon = \{X \in R^6 : \text{dist}(X, \mathcal{O}^*) < \epsilon\}$$
$$\text{dist}(X, \mathcal{O}^*) \triangleq \inf_{Z \in \mathcal{O}^*} \|X - Z\|$$

We now define stability of the orbit $\mathcal{O}^*$ from [11].

Definition 1: The orbit $\mathcal{O}^*$ in (14) is

- stable, if for every $\epsilon > 0$, there is a $\delta > 0$ such that $X(0) \in U_\delta \implies X(t) \in U_\epsilon, \ \forall t \geq 0$.
- asymptotically stable if it is stable and δ can be chosen such that $\lim_{t\to\infty} \text{dist}(X(t), \mathcal{O}^*) = 0$.

The stability characteristics of the hybrid orbit $\mathcal{O}^*$ can be studied by investigating the stability properties of the fixed point $\bar{Y}^*$ in (12), this follows from the following theorem, which is an abridged version of results in the literature - see [3], [16].

Theorem 1: The hybrid orbit $\mathcal{O}^*$ is asymptotically stable if the fixed point $\bar{Y}^*$ is asymptotically stable.

Proof: See the proof of [3, Th. 1], or [16, Th. 2.1 and Corollary 3.2]. ■

The ICPM approach [8] was developed for stabilization of continuous-time orbits of underactuated systems but it can be readily applied to stabilize the hybrid orbit $\mathcal{O}^*$ as it relies on stabilization of the fixed point $\bar{Y}^*$ through application of impulsive inputs. The idea behind the ICPM approach is explained with the help of Fig. 4. The desired hybrid orbit $\mathcal{O}^*$, shown in red, first intersects the Poincaré section S at $\bar{Y}^*$. The application of (I^*, r^*) produces a discontinuous change in the trajectory that lies on S. For a trajectory not on $\mathcal{O}^*$, the discrete-time states $\bar{Y}(k) = \bar{Y}(t_k^-)$ jump to $\bar{Y}(t_k^+)$ due to application of the inputs $I(k)$ and $r(k)$ at time t_k. Hereafter, the devil-stick undergoes torque-free motion under gravity and the next intersection of the continuous-time trajectory with S is denoted by $\bar{Y}(k+1) = \bar{Y}(t_{k+1}^-)$. The control inputs $I(k)$ and $r(k)$ are designed such that they converge to I^* and r^* and $\bar{Y}(k)$ converges to $\bar{Y}^*$ asymptotically as $k \to \infty$.

To apply the ICPM approach, we linearize the map $\mathbb{P}$ given by (9) about $\bar{Y} = \bar{Y}^*$, $I = I^*$ and $r = r^*$ as follows:

$$e(k+1) = \mathcal{A}\, e(k) + \mathcal{B}\, u(k)$$
$$e(k) \triangleq \bar{Y}(k) - \bar{Y}^*, \quad u(k) \triangleq \left[I(k) - I^* \ r(k) - r^*\right]^T \quad (15)$$

where the matrices $\mathcal{A}$ and $\mathcal{B}$ are defined as follows:

$$\mathcal{A} \triangleq \left[\nabla_{\bar{Y}} \mathbb{P}(\bar{Y}, I, r)\right]_{\bar{Y}=\bar{Y}^*, I=I^*, r=r^*}$$
$$\mathcal{B} \triangleq \left[\nabla_I \mathbb{P}(\bar{Y}, I, r) \ \ \nabla_r \mathbb{P}(\bar{Y}, I, r)\right]_{\bar{Y}=\bar{Y}^*, I=I^*, r=r^*} \quad (16)$$

The matrices $\mathcal{A}$ and $\mathcal{B}$ in (16) can be analytically obtained from (9) as follows:

$$\mathcal{A} = \begin{bmatrix} -1 & 0 & 0 & 0 & 0 \\ -g\delta^{*3}s^*/(2\Delta\theta c^*) & -1 & -\delta^* & 0 & 0 \\ 0 & 0 & -1 & 0 & 0 \\ g\delta^{*3}/(2\Delta\theta) & 0 & 0 & 1 & \delta^* \\ g\delta^{*2}/\Delta\theta & 0 & 0 & 0 & 1 \end{bmatrix}$$
$$\mathcal{B} = \begin{bmatrix} -2\Delta\theta c^*/(mg\delta^{*2}) & -(\delta^* gm)/(Jc^*) \\ 0 & -mg^2\delta^{*4}s^*/(2\Delta\theta J c^{*2}) \\ s^*/m & 0 \\ 2\delta^* c^*/m & mg^2\delta^{*4}/(2\Delta\theta J c^*) \\ 3c^*/m & mg^2\delta^{*3}/(\Delta\theta J c^*) \end{bmatrix} \quad (17)$$

where $s^* \triangleq \sin\theta^*$ and $c^* \triangleq \cos\theta^*$. It can be verified that all eigenvalues of $\mathcal{A}$ have a magnitude of unity; this indicates that $\bar{Y}^*$ is marginally stable for $u(k) = 0$. To asymptotically stabilize $\bar{Y}^*$, i.e., to asymptotically stabilize $\mathcal{O}^*$, we present a control design with the help of the following theorem:

Theorem 2: The hybrid orbit $\mathcal{O}^*$ is asymptotically stable under the following discrete feedback

$$u(k) = \mathcal{K} e(k) \quad (18)$$

where the matrix $\mathcal{K}$ is chosen such that $(\mathcal{A} + \mathcal{B}\mathcal{K})$ is Hurwitz.

Proof: Since $\delta^* > 0$ and $\theta^* \in (0, \pi/2)$, it can be shown that $\{\mathcal{A}, \mathcal{B}\}$ is controllable. Thus $\mathcal{K}$ can be chosen such that $(\mathcal{A} + \mathcal{B}\mathcal{K})$ is Hurwitz. The choice of control $u(k)$ in (18) guarantees asymptotic stability of $\bar{Y}^*$, and using Theorem 1 we claim asymptotic stability of $\mathcal{O}^*$. ■

Remark 1: The ICPM approach was first proposed for orbital stabilization of underactuated mechanical systems in [8] where linearization of the Poincaré map was carried out numerically. Here, for the devil-stick juggling problem, a linearized Poincaré map is obtained analytically. This enables us to verify the controllability of the system analytically.

Remark 2: For the control design in (18), the devil-stick rotates by an angle of $(\pi - 2\theta^*)$ between two control actions. Without loss of generality, the control design can be modified such that the stick rotates multiple times during the flight phase; this can be accomplished by simply changing $\Delta\theta = (\pi - 2\theta^*)$ to $\Delta\theta = (q\pi - 2\theta^*), q = 1, 2 \ldots$ in (10).

V. Simulations

In SI units, the physical parameters of the devil-stick are:

$$m = 0.1, \quad \ell = 0.5, \quad J = 0.0021 \quad (19)$$

By choosing $\theta^* = \pi/6$ rad and $\delta^* = 0.5$ sec and using (19) in (13), we get

$$\omega^* = -4.18\,\text{rad/s} \quad \text{h}_\text{x}^* = 0.353\,\text{m} \quad \text{v}_\text{x}^* = 1.414\,\text{m/s}$$
$$v_y^* = -2.45\,\text{m/s} \quad \text{I}^* = 0.565\,\text{Ns} \quad \text{r}^* = 0.030\,\text{m} \quad (20)$$

and the value of h_y^* is chosen arbitrarily as

$$h_y^* = 3.0\,\text{m} \quad (21)$$

Authorized licensed use limited to: Michigan State University. Downloaded on January 05,2023 at 17:22:27 UTC from IEEE Xplore. Restrictions apply.

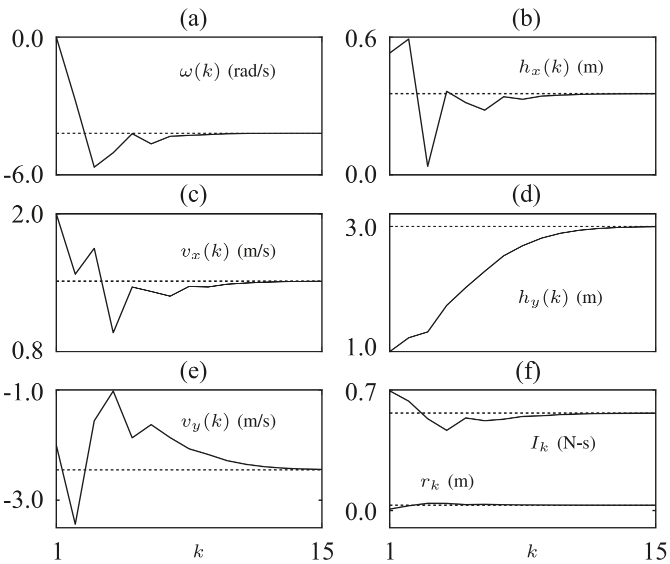

Fig. 5. State variables and control inputs of the devil-stick at sampling instants k, $k = 1, 2, \ldots, 15$ for the initial conditions in (22) and gain matrix in (23).

We assume $\theta(0) = \theta^* = \pi/6$ rad and the initial values of the states variables are chosen as:

$$\begin{aligned} \omega(0) = 0, \quad h_x(0) = 0.53, \quad v_x(0) = 2.0 \\ h_y(0) = 1.0, \quad v_y(0) = -2.0 \end{aligned} \tag{22}$$

It should be noted that the choices in (19), (20) and (21) are identical to that in [9]. The discrete impulsive feedback in (18) is designed by placing the poles of the closed loop system at 0.10, 0.12, 0.30, −0.40 and 0.50; this results in the gain matrix:

$$\mathcal{K} = \begin{bmatrix} -0.001 & 0.226 & 0.183 & 0.003 & -0.012 \\ -0.003 & -0.021 & -0.015 & -0.003 & -0.002 \end{bmatrix} \tag{23}$$

The simulation results are shown in Fig. 5. The discrete state variables $\bar{Y}$ on the Poincaré section S are shown in Figs. 5(a)–(e); the control inputs I_k and r_k are shown in Fig. 5(f). The steady-state values of the states and control inputs, given in (20) and (21), are shown with the help of dotted lines in their respective figures. It can be seen that the state variables and control inputs converge to their steady-state values in approximately $k = 15$ steps. It is clear from the simulation results that the ICPM approach stabilizes the fixed point $\bar{Y}^*$, which implies that the control objective of juggling the devil-stick is achieved.

For visualization, the trajectory of the center-of-mass of the devil stick is shown in Fig. 6. Under the action of gravity, the center-of-mass moves in a parabolic trajectory between control actions and eventually gets juggled between the symmetric configurations (h_x^*, h_y^*) and $(-h_x^*, h_y^*)$.

Remark 3: A two-step control design for devil-stick juggling was proposed in [9]. To stabilize the fixed point of the Poincaré map in (9), a dead-beat design was first utilized to converge ω to ω^*. This resulted in feedback linearization of the residual system and linear control techniques were subsequently used for stabilization of the fixed point. Depending upon initial conditions, the dead-beat controller

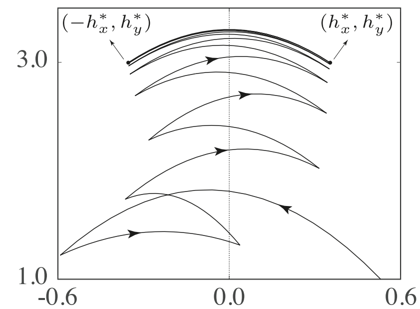

Fig. 6. Trajectory of the center of mass (h_x, h_y) of the devil-stick.

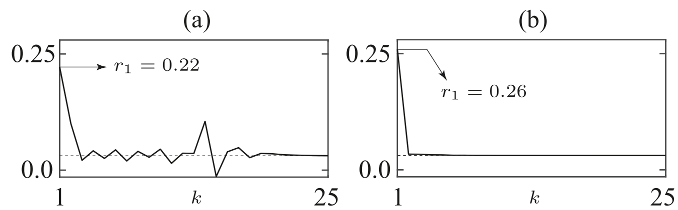

Fig. 7. Comparison of the control input r_k, $k = 1, 2, \ldots, 25$, obtained using the (a) ICPM approach, proposed here, and (b) approach proposed in [9].

may require a large initial control action. Due to constraint on the input, dead-beat convergence may not occur and consequently the linear controller may be rendered ineffective. The ICPM approach proposed here does not suffer from this limitation.

To demonstrate the limitation of the control design in [9], we considered a large value of the initial angular velocity of the devil-stick. In particular, we chose $\omega(0) = -80$ rad/s while keeping all other initial conditions the same as in (22). Furthermore, the controller parameters were not altered. Due to the dead-beat nature of the control design in [9], the controller required $r_1 = r(1) = 0.26$ m, which violates the input constraint $r(k) < \ell/2 = 0.25$. In contrast, the ICPM approach-based control design, presented here, stabilized the desired juggling motion without violating the input constraint. The plots of $r(k)$, obtained using both approaches, are presented in Fig. 7.

To demonstrate robustness of the closed-loop system, we introduced parameter uncertainty, sensor noise and error in the measurement of devil-stick orientation, simultaneously. For the initial conditions and controller gains in (22) and (23), the simulation results are shown in Fig. 8. The values of the length ℓ and inertia J were chosen to be 2.5% and 6.25% less than the values provided in (19) but the steady-state values in (20) were left unchanged. All state variable measurements were corrupted by random noise in the range of ±2.5%; additionally, we introduced a ±2.0 degree error in the measurement of the orientation of the devil-stick. The simulations, which were carried out over a longer duration, indicate stable behavior with ultimate boundedness of the state trajectories.

VI. Conclusion

Juggling a devil-stick is a form of non-prehensile manipulation [12], [13] as it involves manipulation without grasping.

Authorized licensed use limited to: Michigan State University. Downloaded on January 05,2023 at 17:22:27 UTC from IEEE Xplore. Restrictions apply.

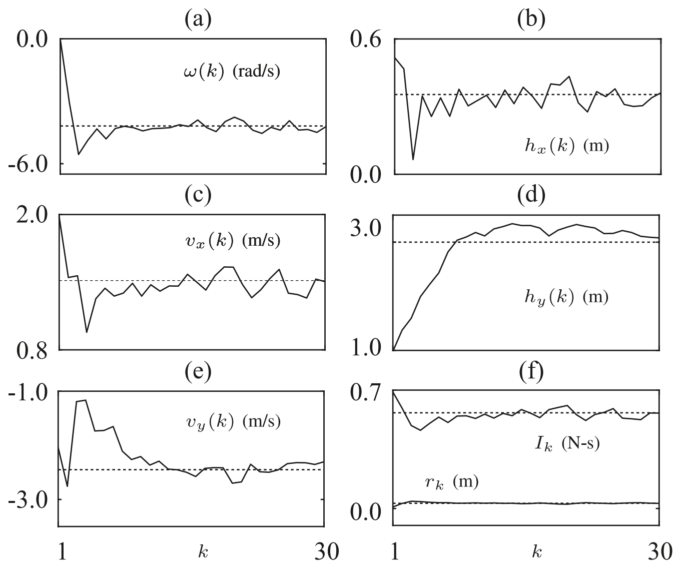

Fig. 8. State variables and control inputs of the devil-stick at sampling instants k, $k = 1, 2, \ldots, 30$ in the presence of parameter uncertainty, sensor noise, and error in the measurement of devil-stick orientation.

Typically, a juggler manipulates the devil-stick by applying intermittent impulsive forces using two hand-sticks. Several different modes of juggling have been documented and top-only idle is the simplest mode for a human juggler. In top-only idle, a devil-stick is juggled between two symmetric configurations about the vertical. With the goal of robotic juggling, we consider the control problem where the impulse of the impulsive force and its point of application are modeled as control inputs. The devil stick represents an underactuated system and its control problem is nontrivial since the inputs are applied intermittently; at all other times, the devil-stick is uncontrolled and undergoes torque-free motion under gravity.

The dynamics of the devil-stick is described by a Poincaré map and stable juggling is equivalent to stabilization of a hybrid orbit, which can be accomplished through stabilization of the fixed point of the Poincaré map. The ICPM approach, recently developed for stabilization of continuous-time orbits of underactuated systems, is a natural choice for control design since the control inputs for the devil-stick are purely impulsive in nature. Utilizing the ICPM approach, the Poincaré map is linearized about the fixed point; this results in a controllable linear discrete-time system. Asymptotic stabilization of the fixed point is achieved using pole-placement. The simplicity and effectiveness of the ICPM approach and its robustness are demonstrated through simulations. Our future work will focus on experimental validation; this includes design of experimental hardware and motion planning and control of the robot end-effector for generating the desired impulsive forces to be applied to the devil-stick.

References

[1] K. Bold *et al.*, "The forced Van der Pol equation II: Canards in the reduced system," *SIAM J. Appl. Dyn. Syst.*, vol. 2, no. 4, pp. 570–608, 2003.

[2] B. Brogliato and A. Z. Rio, "On the control of complementary-slackness juggling mechanical systems," *IEEE Trans. Autom. Control*, vol. 45, no. 2, pp. 235–246, Feb. 2000.

[3] J. W. Grizzle, G. Abba, and F. Plestan, "Asymptotically stable walking for biped robots: Analysis via systems with impulse effects," *IEEE Trans. Autom. Control*, vol. 46, no. 1, pp. 51–64, Jan. 2001.

[4] J. Guckenheimer, K. Hoffman, and W. Weckesser, "The forced Van der Pol equation I: The slow flow and its bifurcations," *SIAM J. Appl. Dyn. Syst.*, vol. 2, no. 1, pp. 1–35, 2003.

[5] HNWpodcasts. (2013). *Five Easy Devil Stick Tricks with Instructions*. Accessed: May 1, 2020. [Online]. Available: https://www.youtube.com/watch?v=Z7Pv-p-nEYo

[6] N. Kant, R. Mukherjee, and H. K. Khalil, "Stabilization of homoclinic orbits of two degree-of-freedom underactuated systems," in *Proc. Amer. Control Conf. (ACC)*, Philadelphia, PA, USA, Jul. 2019, pp. 699–704.

[7] N. Kant and R. Mukherjee, "Impulsive dynamics and control of the inertia-wheel pendulum," *IEEE Robot. Autom. Lett.*, vol. 3, no. 4, pp. 3208–3215, Oct. 2018.

[8] N. Kant and R. Mukherjee, "Orbital stabilization of underactuated systems using virtual holonomic constraints and impulse controlled Poincaré maps," *Syst. Control Lett.*, vol. 146, Dec. 2020, Art. no. 104813.

[9] N. Kant and R. Mukherjee, "Non-prehensile manipulation of a devil-stick: Planar symmetric juggling using impulsive forces," *Nonlinear Dyn.*, vol. 103, pp. 2409–2420, Feb. 2021.

[10] N. Kant, R. Mukherjee, D. Chowdhury, and H. K. Khalil, "Estimation of the region of attraction of underactuated systems and its enlargement using impulsive inputs," *IEEE Trans. Robot.*, vol. 35, no. 3, pp. 618–632, Jun. 2019.

[11] H. K. Khalil, *Nonlinear Systems*, 2nd ed. Upper Saddle River, NJ, USA: Prentice-Hall, 1996.

[12] K. M. Lynch and M. T. Mason, "Dynamic underactuated nonprehensile manipulation," in *Proc. IEEE/RSJ Int. Conf. Intell. Robots Syst. (IROS)*, vol. 2. Osaka, Japan, 1996, pp. 889–896.

[13] K. M. Lynch and T. D. Murphey, "Control of nonprehensile manipulation," in *Control Problems in Robotics*, Heidelberg, Germany: Springer, 2003, pp. 39–57.

[14] F. B. Mathis, R. Jafari, and R. Mukherjee, "Impulsive actuation in robot manipulators: Experimental verification of pendubot swing-up," *IEEE/ASME Trans. Mechatronics*, vol. 19, no. 4, pp. 1469–1474, Aug. 2014.

[15] S. Nakaura, Y. Kawaida, T. Matsumoto, and M. Sampei, "Enduring rotary motion control of devil stick," *IFAC Proc. Vol.*, vol. 37, no. 13, pp. 805–810, 2004.

[16] S. G. Nersesov, V. Chellaboina, and W. M. Haddad. A generalization of Poincaré's theorem to hybrid and impulsive dynamical systems," in *Proc. Amer. Control Conf.*, vol. 2. Anchorage, AK, USA, 2002, pp. 1240–1245.

[17] R. Ronsse, P. Lefevre, and R. Sepulchre, "Rhythmic feedback control of a blind planar juggler," *IEEE Trans. Robot.*, vol. 23, no. 4, pp. 790–802, Aug. 2007.

[18] R. G. Sanfelice, A. R. Teel, and R. Sepulchre, "A hybrid systems approach to trajectory tracking control for juggling systems," in *Proc. 46th IEEE Conf. Decis. Control*, New Orleans, LA, USA, 2007, pp. 5282–5287.

[19] S. Schaal and C. G. Atkeson, "Open loop stable control strategies for robot juggling," in *Proc. IEEE Int. Conf. Robot. Autom.*, Atlanta, GA, USA, 1993, pp. 913–918.

[20] A. Shiriaev, A. Robertsson, L. Freidovich, and R. Johansson, "Generating stable propeller motions for devil stick," in *Proc. 3rd IFAC Workshop Lagrangian Hamiltonian Methods Nonlinear Control*, 2006, pp. 105–110.

[21] A. Zavala-Rio and B. Brogliato, "On the control of a one degree-of-freedom juggling robot," *Dyn. Control*, vol. 9, no. 1, pp. 67–90, 1999.

Authorized licensed use limited to: Michigan State University. Downloaded on January 05,2023 at 17:22:27 UTC from IEEE Xplore. Restrictions apply.